Boundary-Forced Planetary Waves: A Simple Model Mid-Ocean Response to Strong Current Variability

D. E. HARRISON

Department of Earth and Planetary Sciences, Massachusetts Institute of Technology, Cambridge 20139

A. R. ROBINSON

Center for Earth and Planetary Physics, Harvard University, Cambridge, MA 02139

(Manuscript received 17 July 1978, in final form 1 March 1979)

ABSTRACT

A simple linear model of the barotropic basin response to forcing imposed along the northern boundary is described. The dependence on latitude of the response may include oscillatory behavior or not, depending on whether the forcing frequency is smaller or greater than the fundamental free basin mode frequency. When oscillatory behavior is found, the forced solution may resemble oceanic mesoscale eddies. The relevance of this simple model to a description of the eddy fields of several mesoscale resolution general ocean circulation numerical experiments is examined. It is found that a single term of the analytical solution can very well describe the numerically produced eddy fields, away from the regions of strong currents. The possibility that this general mechanism might account for the existence of mesoscale eddies in the ocean is briefly discussed.

1. Introduction

A variety of generation mechanisms for the mid-ocean mesoscale eddy field have been proposed. They include direct driving by time-dependent surface forcing and mid-ocean baroclinic instability as well as indirect processes like mean-flow interaction with topography, nonlinear energy cascades and energy import from distant unstable regions (see MODE Group, 1978). However, there is growing evidence that the Gulf Stream current, extension, and recirculation system may play an important role in North Atlantic eddy energetics (Schmitz, 1977; Dantzler, 1977). In addition, the analog model Gulf Stream current systems in mesoscale resolution numerical ocean circulation experiments appear generally to act as eddy energy production regions that export to the open ocean the energy required to maintain whatever eddy field exists there (Robinson *et al.*, 1979). Harrison and Robinson (1978) have shown that for one numerical experiment the transport process to the open ocean is pressure work, but the generality of this result is not known at this time. To understand the behavior of various possible energy transport mechanisms thus appears to be an important dynamical problem.

In this paper we describe a very simple model for the far field basin response to energy radiated away from a time-dependent northern current system. This "meander-induced forcing" (MIF) model enables investigation of the circumstances necessary for a time-dependent current to drive mesoscale eddy-like motions in the open ocean by parameterizing the net result of the presumably nonlinear processes in the strong transient current region as an imposed boundary condition on the northern side of the basin. The dynamics are linear and barotropic, the basin is rectangular and the bottom is flat. It is found that the existence of eddy-like driven motions in the basin interior depends on the basin parameters and forcing frequency. The spatial structure of the northern boundary motion determines the amplitudes of eddy-like and trapped terms in the solution, but generally not their existence.

The solution of this MIF problem is applied to a study of the transport eddy flow away from strong current regions of several mesoscale resolution numerical ocean general circulation experiments. In the single gyre calculations examined, the numerically produced eddy fields compare favorably with the possible eddy-like terms in the MIF solution.

Other linear boundary forced calculations have been carried out. Ivanov (1969) studied several systems, including one similar to that reported here except that it was forced along the western boundary. Given the meandering character of the numerical experiment currents, western forcing is not an appropriate model for describing these flows, but his western boundary forced basin case is mathemati-

0022-3670/79/050919-11$06.75

cally similar to ours. Flierl *et al.* (1975) have examined the behavior of semi-infinite domains driven by boundary forcing, and found that the existence of eddy-like motions depends on the values of β and forcing frequency and on westward phase propagation of the boundary motion; conditions different than those obtained here for the finite basin. Pedlosky (1977) has pointed out that the presence of mean currents in a semi-infinite domain can affect the ability of a given forcing to drive eddy-like behavior. The applicability of linear theory to ocean mesoscale eddies is, of course, questionable, but the results reported here will be seen to be relevant to the numerical calculations. Furthermore, other numerical calculations have shown that some linear wave propagation properties appear to be relevant to certain types of nonlinear motions (Rhines, 1977). It also seems desirable to begin analytical studies with as simple a model as might be relevant.

The MIF problem is described and the properties of its solution examined in Section 2. In Section 3 the eddy transport fields of the above EGCM experiments are compared with the MIF solutions. The results of this comparison are discussed and some remarks concerning the possibility of ocean eddy generation based on these MIF ideas are offered in Section 4.

2. The meander-induced forcing model

The basic model system is that of a homogeneous fluid on a β-plane contained vertically between two flat rigid surfaces, bounded on the east, south and west by rigid walls, subject to a linear drag law, and driven by imposing the streamfunction on the northern wall. The linear model equations are

$$\left.\begin{aligned} &\nabla^2 \frac{\partial \psi}{\partial t} + \beta \frac{\partial \psi}{\partial x} = -R\nabla^2\psi && \text{in} \quad [0,a] \times [0,b] \\ &\psi = 0 && \text{on} \quad x = 0, a; y = 0 \\ &\psi(x,b,t) = \mathrm{Re}[e^{i\omega t} f(x)], && \quad f(0) = f(a) = 0 \end{aligned}\right\}, \tag{1}$$

and the end-point values of f are zero in order to conserve mass. If we scale x, y, t by $a, a, 1/\omega$, respectively, the nondimensional form of (1) is

$$\left.\begin{aligned} &\nabla^2 \frac{\partial \psi}{\partial t} + 2\pi M \frac{\partial \psi}{\partial x} = -\delta\nabla^2\psi && \text{in} \quad [0,1] \times \left[0, \frac{b}{a}\right] \\ &\psi = 0 && \text{on} \quad x = 0, 1; y = 0 \\ &\psi\left(x, \frac{b}{a}, t\right) = \mathrm{Re}[e^{it} f(ax)], && \quad f(0) = f(a) = 0 \end{aligned}\right\}, \tag{2}$$

where the nondimensional parameters

$$M \equiv \frac{\beta a}{2\pi\omega} \quad \text{and} \quad \delta \equiv \frac{R}{\omega}$$

have been introduced.

The equilibrium forced solution to (2) is found by separating variables and using a sine series to satisfy the north wall-boundary condition.

$$\psi^{ND}(x,y,t) = \mathrm{Re}\{e^{(it-\Delta x)} \sum_{m=1}^{\infty} C_m \sin m\pi x Y_m(y)\}, \tag{3a}$$

where

$$\Delta = M\pi\left(\frac{\delta - i}{\delta^2 + 1}\right), \tag{3b}$$

$$Y_m(y) = \frac{\sin ky}{\sin k\,\frac{b}{a}}, \tag{3c}$$

$$k^2 = -\pi^2 m^2 - \Delta^2, \tag{3d}$$

$$C_m = 2\int_0^1 f(x) \sin m\pi x e^{\Delta x} dx. \tag{3e}$$

Because of the non-zero bottom drag, Δ and k^2 are complex in general, but the inviscid limit, $\delta = 0$, is simpler:

$$\psi^{ND}(x,y,t) = \mathrm{Re}\{e^{i(M\pi x + t)} \sum_{m=1}^{\infty} C_m \sin m\pi x Y_m(y)\}, \tag{4a}$$

since

$$\Delta = -iM\pi, \quad k^2 = \pi^2[M^2 - m^2] \tag{4b}$$

and

$$Y_m(y) = \begin{cases} \dfrac{\sin ky}{\sin k\,\dfrac{b}{a}}, & \text{if } k^2 > 0 \\ \dfrac{\sinh|k|y}{\sinh|k|\,\dfrac{b}{a}}, & \text{if } k^2 < 0 \\ \dfrac{by}{a}, & \text{if } k^2 = 0. \end{cases} \quad (4c)$$

a. The inviscid solution

When $\delta = 0$, Eq. (4) describes the MIF solution. Each term of the series is a plane wave, with westward phase speed of $1/M\pi$ ($2\omega^2/\beta$ dimensionally), times a modulating function of x and y. The structure of the modulation in x is simply $\sin m\pi x$ for the mth term, but the y modulation is more complicated. When $m < M$, it is seen that $k^2 > 0$ and so $Y_m(y) \propto \sin ky$, while for $m > M$, $k^2 < 0$, and so $Y_m(y) \propto \sinh|k|y$. It will be convenient to refer to terms according to their qualitative structure in the y direction; when $Y_m(y)$ has at least one interior zero the term will be classed *eddy-like* and will otherwise be classed *trapped*. An eddy-like term has closed interior streamlines and a trapped term does not.

Clearly, terms for which $k^2 < 0$ are always trapped, as $Y_m(y)$ decreases monotonically from 1 at the northern boundary to zero at the south. As m increases they become more and more confined near the northern boundary. Whether or not a term with $k^2 > 0$ will be eddy-like is determined by kb/a greater or less than π. It is easily seen that we must have

$$M > \left[\left(\frac{a}{b}\right)^2 + 1\right]^{1/2} \quad (5)$$

in order for there to be at least one eddy-like term in (4a). The general constraint is that

$$\left[\left(\frac{a}{b}\right)^2 + m^2\right]^{1/2} < M \quad (\text{and } m < M) \quad (6)$$

if the mth term is to be eddy-like. Given a pair of eddy-like terms ψ_m and $\psi_n (m < n)$, ψ_m will have the more complex structure in y and ψ_n the more complex structure in x.

The above remarks are independent of the spatial structure of the forcing function $f(x)$. Of course, $f(x)$ determines the amplitude of each term in Eqs. (4) through (3e), but the presence or absence of eddy-like terms in (4) does not depend on $f(x)$. In order for Eq. (4) to converge the C_m must drop off at least as fast as m^{-1} for m greater than some integer m^+, and for smooth $f(x)$ it is reasonable to assume more rapid decrease. Since the trapped modes generally go exponentially to zero as $y \to 0$, it seems reasonable to assume that the character of the solution well away from the northern boundary may be largely determined by the eddy-like terms in the series. For a physical system with only a few eddy-like terms much can be inferred about the possible "far field" motions even if $f(x)$ is poorly known. If many eddy-like terms are possible, it is necessary to know $f(x)$ and evaluate the C_m coefficients in order to determine the structure of the eddy-like solution. We note in passing that $f(x) = e^{iM\pi x} \sin n\pi x$ will lead to $C_m = \delta_{mn}$.

If the forcing frequency is such that there exists at least one $m < M$ for which kb/a is a multiple of π, then this term of the series will have infinite amplitude because the normalizing factor in $Y_m(y)$ is infinite. This resonance occurs at the frequencies of the linear free oscillations of the corresponding closed basin. There are interesting relationships between certain eddy-like terms and these free oscillations.

The free oscillations are the solutions of Eq. (1) with $\psi = 0$ on all four sidewalls. The dimensional solution for the (m,n) mode is

$$\psi_{mn}(x,y,t) = \begin{Bmatrix} \text{Re} \\ \text{Im} \end{Bmatrix} \left[\exp\{i[(\beta x/2\omega_{mn}) + \omega_{mn} t]\} \times \sin\frac{m\pi x}{a} \sin\frac{n\pi y}{b} \right], \quad (7a)$$

where

$$\omega_{mn} = \frac{\beta a}{2\pi}\left[\left(\frac{a}{b}\,n\right)^2 + m^2\right]^{-1/2}. \quad (7b)$$

From (7b) the highest frequency is that of the gravest mode and is

$$\omega_{11} = \frac{\beta a}{2\pi}\left[\left(\frac{a}{b}\right)^2 + 1\right]^{-1/2}$$

or

$$M_{11} = \left[\left(\frac{a}{b}\right)^2 + 1\right]^{1/2}.$$

If time is scaled by ω_{mn}^{-1} and length by a, the nondimensional form of (7a) is

$$\psi_{mn}^{ND} = \begin{Bmatrix} \text{Re} \\ \text{Im} \end{Bmatrix} \left[\exp[i(M_{mn}\pi x + t)] \times \sin n\pi x \sin\frac{a}{b}\, m\pi y \right], \quad (8)$$

which bears obvious resemblance to the eddy-like terms of (4).

Several points should be noted. From (7b) and (5) it is seen that the forcing frequency must be smaller than the fundamental basin mode frequency ($\omega < \omega_{11}$) if there are to be eddy-like terms in the solution (4).

For $\omega = \omega_{mn}$ the mth term in (4) is identical in structure to that of the (m,n) mode and its amplitude is infinite. In general, however, MIF eddy-like terms are distinct from the free modes of the MIF basin. Comparison of (4) and (8) reveals that eddy-like MIF terms may have a range of possible spatial structures while maintaining the same period and westward phase speed; basin modes have a specified spatial form for each period satisfying the dispersion relation (7b).

Each eddy-like term has an "equivalent basin mode," which is a free mode of a basin of dimension $a \times b^+$, that is identical in the $a \times b$ basin to the eddy-like term. Generally, b^+ is the smallest number greater than b for which kb^+/a is an integer multiple of π. If kb/a is an integer multiple of π then one is back to the resonance case, $\omega = \omega_{mn}$, discussed above. These inviscid MIF eddy-like terms constitute a class of basin motions, including the free-basin modes as a subset, that may prove useful for the description of ocean mesoscale motions.

b. The solution including viscous effects

The wavelike multiplicative part of each term now has the form

$$\exp\{i[t + M\pi x/(\delta^2 + 1)]\} \times \exp[-M\pi\delta x/(\delta^2 + 1)] \quad (9)$$

and the $Y_m(y)$ part is proportional to

$$\sin\left\{-\pi^2\left[m^2 + \left(\frac{\delta - i}{\delta^2 + 1}\right)^2 M^2\right]\right\}^{1/2} y. \quad (10)$$

Rather than extensively discuss the behavior of the solution, it will suffice to observe that the introduction of a linear drag increases the westward phase speed to $(\delta^2 + 1)/M\pi$, leads to a trapping length scale of $(\delta^2 + 1)/\delta M\pi$ away from the western boundary, makes $Y_m(y)$ complex in general and leads to finite response to forcing at a basin mode frequency. For small δ, $Y_m(y)$ behaves basically as described above, but δ of order one or greater can lead to considerably different characteristics.

c. Baroclinic effects

Although the homogeneous fluid case appears most relevant to the numerical model eddy flows to be discussed in Section 3, the effects of stratification are of interest. The simplest way stratification can be introduced is through linear quasi-geostrophic dynamics. The equation for conservation of quasi-geostrophic potential vorticity is separated into a steady vertical structure equation that is an eigenvalue problem for the vertical modes of the flow, and a set of equations for the evolution of the horizontal fields of the different modes are derived. Stratification effects enter the horizontal equation only through the vertical equation eigenvalue, corresponding to the inverse radius of deformation of that mode (see, e.g., Philander 1978). The horizontal equation for the ith vertical mode is identical in form to equation (1) except $\nabla^2 \to \nabla^2 - \lambda_i^2$, where λ_i is the inverse radius of deformation, and the forcing boundary condition is now the projection of the total boundary condition onto the ith mode. Using zero boundary conditions[1] except on the northern boundary leads to a solution for the ith mode that is identical to that of (4) except that $k^2 = \pi^2[M^2 - (\lambda_i a/\pi)^2 - m^2]$. The quantity $M^* \equiv [M^2 - (\lambda_i a/\pi)^2]^{1/2}$ replaces M in all remarks about the existence of eddy-like terms.

3. Comparison with EGCM results

In this section we examine the extent to which the simple MIF model is able to describe the transport eddy fields, away from strong currents, of the single gyre numerical experiments of Holland and Lin (1975), Robinson *et al.* (1977), and Holland (1978). An issue immediately arises in how to select the quantities needed for input to the MIF model. The east–west extent of the basin a and variation with latitude of the Coriolis parameter β are no problem but the determination of the north–south extent of the MIF basin (b), the spatial structure of the streamfunction field as a function of time at $y = b$, and the frequencies of interior eddy motions is not so straightforward. The procedures here adopted are (i) to take ω as the dominant reported eddy frequency; (ii) estimate b from examination of published flow fields and, where available, plots of energy transformations; and (iii) adopt an analysis procedure which does not require knowledge of $f(x)$. It is not possible to estimate the structure of the forcing functions from published data. Instead the possible eddy-like MIF terms are evaluated and compared to the numerical model eddy fields to see if a simple linear combination of MIF eddy-like terms can describe the observed eddies.

Table 1 presents the EGCM basin values as well as the deduced MIF parameters. In every case, the north–south dimension of the EGCM basin (b^*) is significantly greater than b. No error bars are available for forcing frequency values except for the experiment of Robinson *et al.* (1977). The experiment and eddy fields of each calculation are briefly described before the meander-induced forcing terms are introduced.

[1] This is not strictly correct (McWilliams, 1977) but the results of Flierl (1977) suggest that the solution with homogeneous boundary conditions can in certain cases be qualitatively satisfactory.

TABLE 1. Numerical experiment basin and eddy MIF parameters.

Experiment	a (cm)	b^* (cm)	b (cm)	β ($cm^{-1}\ s^{-1}$)	R (s^{-1})	ω (s^{-1})	M
RHMS	2×10^8	2×10^8	1.3×10^8	1.87×10^{-13}	*	$1.9 \pm 0.05 \times 10^{-6}$	3.1 ± 0.1
H/L.1	1×10^8	1×10^8	0.7×10^8	2.0×10^{-13}	**	1.1×10^{-6}	2.8
H/L.3	1×10^8	1×10^8	0.5×10^8	2.0×10^{-13}	**	2.6×10^{-6}	1.2
H/L.4	1×10^8	1×10^8	0.5×10^8	2.0×10^{-13}	**	2.3×10^{-6}	1.4
H/L.7	2×10^8	2×10^8	1.8×10^8	2.0×10^{-13}	**	4.5×10^{-6}	1.4
H.1	1×10^8	1×10^8	0.7×10^8	2.0×10^{-13}	**	1.1×10^{-6}	2.8

* Nonlinear drag law.
** No bottom drag.

a. Robinson, Harrison, Mintz and Semtner (1977)

In this primitive equation, five level, wind and thermally forced experiment (hereafter called RHMS) the primary energy source of the eddies is the conversion of kinetic energy of the mean flow into mean eddy kinetic energy. The northern current system and its vigorously meandering near field occupy the northern third of the basin. In the southern two thirds of the domain, away from the intense northern currents, the eddy motion is quite barotropic and the relevance of the model can be examined. Fig. 1a shows the eddy transport streamfunction at two times.

From Table 1, $M = 3.1 \pm 0.1$ and $b \sim 2/3b^* = 2/3a$. Using the criterion $[(a/b)^2 + m^2]^{1/2} < M$ for eddy-like terms in (4) reveals that $m = 1$ and 2 are the only eddy-like terms for the MIF basin. Fig. 1b presents the $m = 1$ term for comparison with the numerical model eddy field; $Y_1(y)$ and $\cos(M\pi x + t)\ \sin\pi x$ are displayed adjacent to the EGCM eddy maps. The agreement between the $m = 1$ MIF term and numerical eddy field is excellent in wavelength, phase speed and spatial characteristics. The other eddy-like term, $m = 2$ does not resemble Fig. 1a at all. Some spatial details are, of course, not completely described by the $m = 1$ term; it is smoother and more regular than the EGCM field.

b. Holland and Lin (1975)

Each of these experiments is a wind forced, two-layer primitive equation system with physically different parameters.

1) EXPERIMENT 1[2]

The basin-integrated energetics of this system reveal that the eddy field is driven by conversion of potential energy into mean eddy kinetic energy. The northern current system, the near-field and the strong energy conversion region involve most of the northern half of the basin. The northern basin eddies are quite different from those in the southern half of the domain, as is suggested by Fig. 2a. In the southern area the eddies are quite barotropic and it is plausible to compare them with the theory.

The Table 1 values are $M \approx 2.8$, $b \approx 1/2b^* = 1/2a$, and show that two eddy-like terms exist in (4). Fig. 2b presents $Y_2(y)$ and $\cos(M\pi x + t) \times \sin 2\pi x$, in the manner of Fig. 1b, for comparison with the southern eddies. The qualitative agreement is again very good but there are occasionally limited areas of the basin where the sign of the solution is incorrect (Day 2120 and 2150). The $m = 1$ term does not resemble the overall structure of the southern eddies. The extent to which a small $m = 1$ contribution would account for these small differences has not been evaluated.

2) EXPERIMENTS 3 AND 4

The eddy flow in these calculations is driven by a combination of conversion of kinetic energy of the mean flow and of potential energy, and they are flows of higher external Reynolds number than any of the other Holland and Lin experiments (see Table 1, RHMS). The flows of these experiments are also different from all other calculations, in that there is really no "far field"; the strong northern current systems cover at least the northern half of the basin in the mean and strong meandering behavior extends instantaneously even further to the south (Figs. 2 and 4, Holland and Lin, 1975, Part II). It is not clear that the model should be relevant for these cases, but we consider the motion in the southern half of the basin in the interest of completeness. Figs. 3a and 4a show the eddy streamfunction fields and reveal that the eddies are of basin scale meridionally.

From Table 1 it is found that $M \approx 1.2$ and $b \approx 1/2b^* = 1/2a$ for experiment 3 and $M \sim 1.4$ with $b \approx 1/2b^* = 1/2a$ for experiment 4. Thus there will be no eddy-like terms for the MIF basin for either experiment, which is in accord with the observed eddies. However, the $m = 1$ term of (4) is shown in Figs. 3b and 4b, in the manner of Fig. 1b, for comparison. Fig. 3b was evaluated using a value of ω

[2] The results of the single gyre Holland (1978) calculation are very much like those of this case, and all remarks made here apply equally to that experiment.

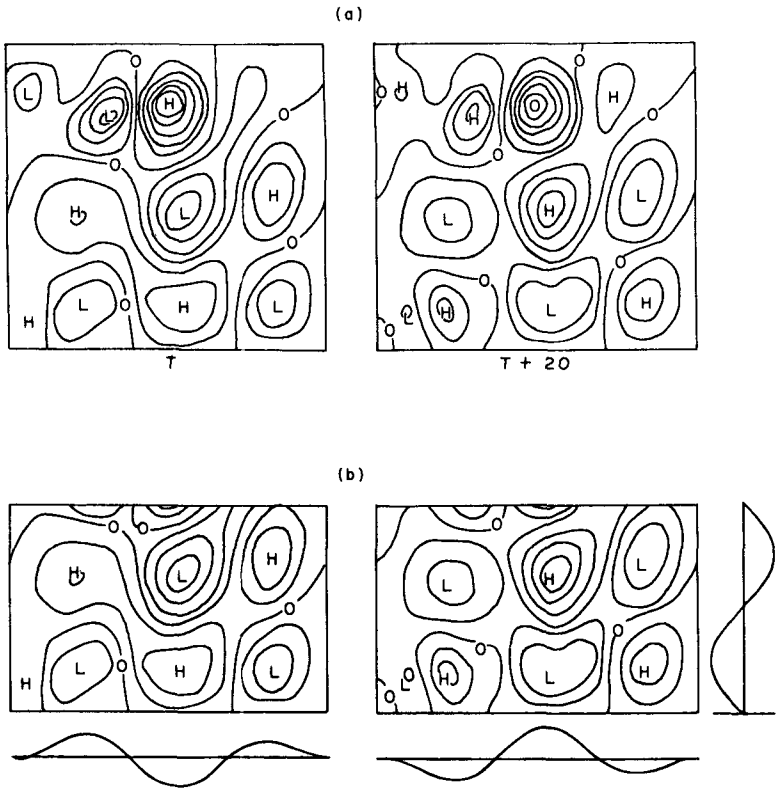

FIG. 1. (a) Eddy streamfunction field snapshots from RHMS, 20 days apart. (b) Comparison of $m = 1$ MIF term with RHMS eddy streamfunction fields in the MIF basin: $Y_1(y)$ at far right, $\cos(M\pi x + t)\sin\pi x$ at bottom.

about 10% smaller than that reported by Holland and Lin, and shows excellent correspondence between the MIF term and EGCM field. With the reported ω value the westward phase speed of the MIF solution is about 10% slower than that of the EGCM field and there is a similar magnitude wavelength difference. Given the quality of the Fig. 6b fit, it is suggested that the reported ω value may be larger than the eddy value; no error estimates on ω are reported. The Fig. 4b correspondence is also excellent for the single EGCM field comparison possible, but additional EGCM maps would be needed for a phase speed comparison.

3) EXPERIMENT 7

No information is given about the energetics of this flow. There are strong eddies only in the northern current system and they are quite baroclinic. From the published data it is difficult to define the characteristics of the weak (~16-day period), large-scale interior eddy field. However, Lin (1974) presents a time series of eddy streamfunction maps which is shown as Fig. 5a. The contour interval is sufficiently large that only the phase propagation of the $\psi = 0$ contour is clear in the interior system.

From Table 1, $b \approx 0.7b^* = 0.7a$, $M \approx 1.4$, and there should be no eddy-like term. As before, it is worth comparing the model eddy flow with the $m = 1$ MIF term, which is done in Fig. 5b in the manner of Fig. 1b. The large-scale comparison is good, but there are smaller scale, irregular features with no MIF term counterpart. With the available information it is not possible to determine whether the small scale structure might have the longer period of the strong current system eddies, and correspond to a different MIF term or terms. The MIF term presented is apparently able to account for a significant amount of the general structure of the model eddy field.

4. Summary and discussion

a. The MIF model and numerical experiments

1) NUMERICAL MODEL EDDY FLOWS

The properties of the full domain EGCM eddy fields need to be considered to put the MIF ideas and the results of Section 3 in perspective. Several types of eddy flows are observed: some experiments have distinct eddies in both the MIF basin and the strong current region (Holland and Lin #1, Holland #1, RHMS), others have eddies of full basin scale and so lack distinct MIF basin eddies (Holland

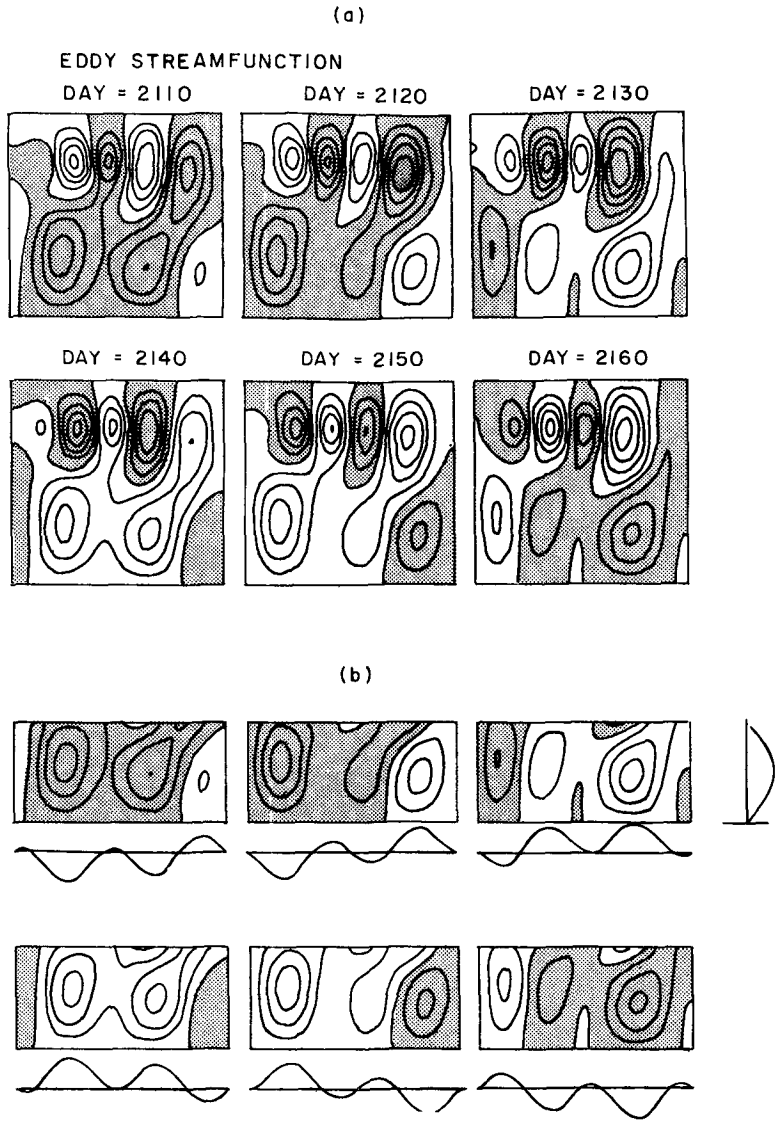

FIG. 2. (a) Eddy streamfunction field snapshots from Holland and Lin #1, 10 days apart. (b) Comparison with $m = 2$ MIF term, as in Fig. 1b.

and Lin #3, #4) and one has distinct strong current region eddies in addition to a basin scale eddy field (Holland and Lin #7). Recall that the MIF basin is the subregion of the full domain obtained by eliminating that northern part of the basin in which strong currents, local eddy energy sources, and nonlinear effects are thought to be important. Generally, the dominant eddy frequency is the same in both the strong current and MIF basin regions, but Holland and Lin #7 has two distinct frequencies. In certain cases the eddy field bears some resemblance to a basin mode of the full domain.

The eddy flow in these experiments is determined by the competition between a number of energetic processes: eddy-mean flow interaction, eddy buoyancy work, mean flow advection of eddy energy, eddy-eddy interaction, eddy pressure work energy transport and dissipation (Harrison and Robinson, 1978). Presumably, the eddy flow that is best able to simultaneously extract energy from the mean flow and minimize dissipation is the one that will dominate in the statistical equilibrium of the system. Whether this equilibrium eddy flow will be of simple or complex spatial and temporal characteristics cannot now be determined *a priori*. For the MIF theory to apply it is necessary that the energy budgets of the subregion of the basin away from the strong northern currents be, basically, quite simple; boundary pressure work transport must be the energy source, with dissipation providing the necessary sink. Harrison and Robinson (1978) have shown that the RHMS flow does have this sort of

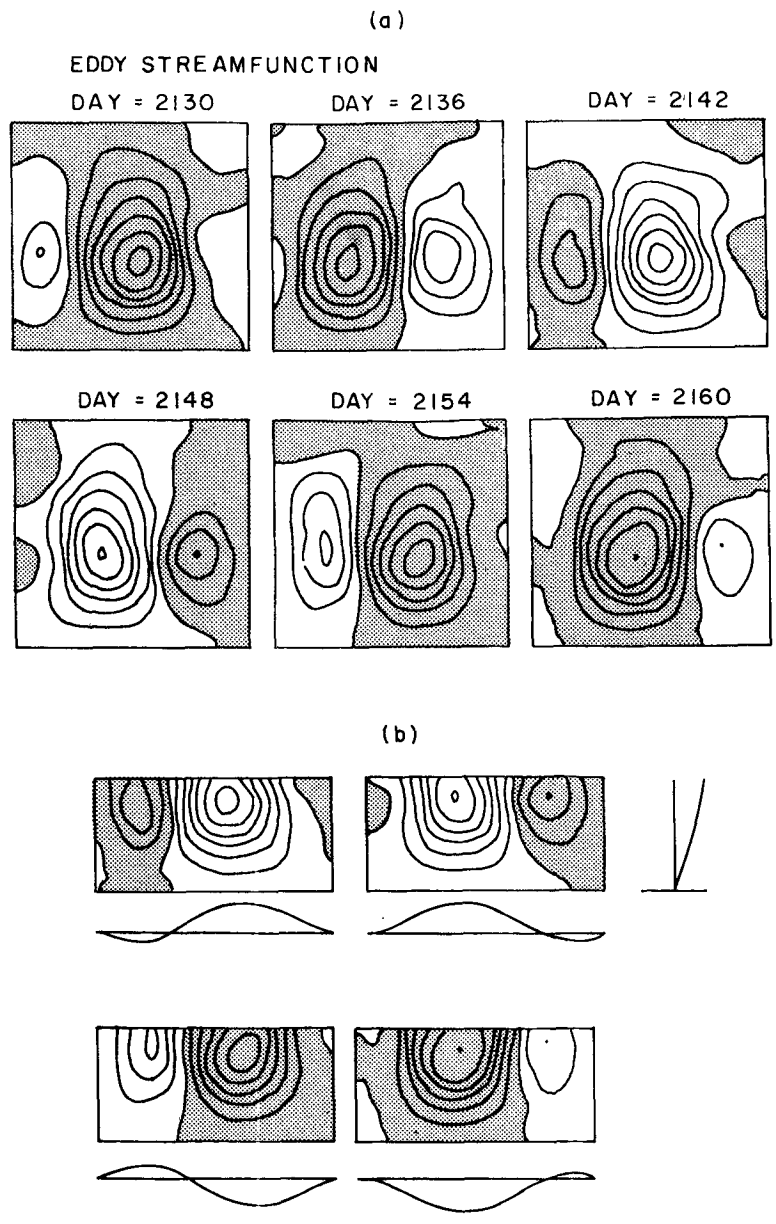

FIG. 3. (a) Eddy streamfunction field snapshots from Holland and Lin # 3, 6 days apart. (b) Comparison with $m = 1$ MIF term, as in Fig. 1b.

energy balance in the Interior region, but detailed analyses of the other experiments are not available.

2) COMPARISON OF MIF THEORY WITH MODEL EDDY FLOWS

In each EGCM flow a single inviscid barotropic MIF eddy-like term, or the $m = 1$ term when no eddy-like terms exist in the solution, has been found to satisfactorily describe the east–west and north–south wavelength and pattern evolution of the EGCM transport streamfunction in what we have defined to be the MIF basin.

The inviscid theory appears to satisfactorily account for the MIF region eddies because viscous effects are relatively small in these flows. If a decay time estimate for these lateral eddy viscosity experiments is estimated from $R \approx 2\pi^2 A/L^2$, where L is an eddy diameter and A is the eddy viscosity, then $\delta \lesssim 10^{-1}$ for all the EGCM cases. The correction to an inviscid eddy-like term due to viscous effects is thus quite small, since the wavenumber and phase speed of the zonally propagating part of the solution (9) depend on δ^2 to the lowest order and the meridional structure is generally also only weakly dependent on δ when δ is small.

The absence of viscous effects in the kinematics should not be misunderstood to mean that the MIF region eddies are free solutions like basin modes; these are forced motions. It is our belief that energy input and dissipation are essential features of these circulations, because the models are integrated forward for so many years that all free oscillations associated with initial conditions will have been damped out. Again only for RHMS are details available, but it is known for that flow that the Interior region eddies have an approximate e-folding time of about three eddy periods due to dissipation. This situation exists even though viscous terms are smaller than the leading terms in the instantaneous momentum and vorticity equations by at least-order Rossby number ($2U_0/f_0L$). Of course, if the flow is forced near an MIF resonance frequency, the smallness of δ ensures that the response will resemble a free mode (see Section 2a).

The MIF theory is not a complete dynamical theory for EGCM eddies because it does not include the strong current region. Some work that attempts to predict the character of strong current region eddies has recently been described by Haidvogel and Holland (1978). They have had some success in predicting the gross characteristics of the strong current region eddies of some of Holland's 1978 experiments, by computing the most unstable eigenfunction of a linear instability analysis of a meridional section of the instantaneous flow. For the one overlapping case between their experiments and those considered here, (Holland #1), they predict the observed period very well. However, no interior eddy field is predicted; our work suggests that this is due to the lack of an enclosed basin in their analysis.

Before closing this section, it should be noted that the multiple gyre EGCM calculations of Holland and Lin (1975), Semtner and Mintz (1977) and Holland (1978) have not been included in this study since, for none of these calculations, is a time series of eddy transport streamfunction available with good eddy frequency information. For double gyre cases the theory would have to be generalized to include internal forcing (unless the gyres could be treated independently—one forced from the north and one from the south), and some cases are simply too geometrically complex.

b. The MIF process and the ocean

It is of interest to examine briefly some of the implications of these MIF ideas to the question of the generation of mid-ocean mesoscale eddies. We shall evaluate the forcing periods required by this MIF theory to produce eddies in an idealized North Atlantic basin, see how these periods are changed when stratification is very simply included and then offer a few remarks about other processes that may affect these simplest results. The remarks offered here are intended to give some insight into the qualitative predictions of the MIF ideas—when long or mesoscale wavelength energy can be radiated away from a region of time-dependent currents into a quiescent, flat bottom region—using values roughly appropriate to the North Atlantic.

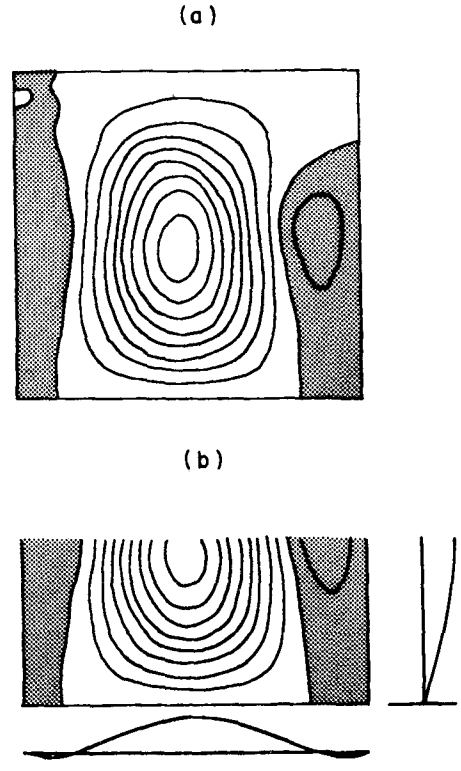

FIG. 4. (a) Eddy streamfunction snapshot from Holland and Lin #4. (b) Comparison with $m = 1$ MIF term, as in Fig. 1b.

1) MIF THEORY ESTIMATES

Consider first the conditions necessary to force eddy-like motions in a 5000 km square basin at mid-latitude ($\beta = 2 \times 10^{-13}$ cm^{-1} s^{-1}) according to the inviscid barotropic MIF model (Section 2a). From (4) and (5) it is seen that an eddy-like term of meridional basin scale is possible only for forcing at periods longer than ~7 days. A meridional width comparable to those that have been observed (~300 km) requires forcing periods longer than ~80 days.

The approximate linear quasi-geostrophic results for forced baroclinic motions (Section 2c), using the basin parameters given above and with MODE-1-type radii of deformation are quite different. Because $\lambda_i a/\pi \gtrsim 40$ for all baroclinic modes, much longer forcing periods are required to drive eddies of a given meridional scale. For the first baroclinic

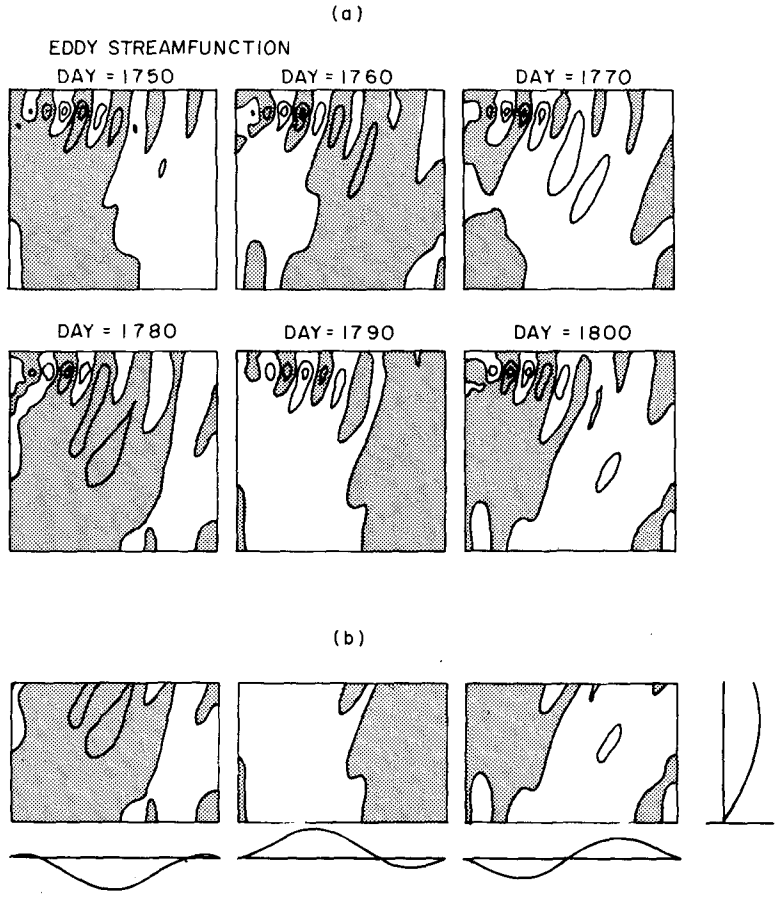

FIG. 5. (a) Eddy streamfunction snapshots from Holland and Lin #7, 10 days apart. (b) Comparison with $m = 1$ MIF term, as in Fig. 1b.

mode, forcing at ~200-day periods is necessary to produce any eddy-like term at all, and ~300-day periods are needed to get ~300 km meridional width.

The effects of viscosity on the barotropic solution (Section 2B) are determined by the magnitude of the ratio of inverse decay time scale to forcing frequency. If the inverse decay time is taken to be $10^{-7}s^{-1}$, then an east-west trapping scale of ~50 km is found for 1-year period forcing and of ~500 km for one month period forcing. Shorter (longer) inverse decay times lead to shorter (longer) trapping scales for forcing of a given period. Although there is considerable uncertainty about how to model dissipative mechanisms in the ocean, this simple estimate suggests that eddies of observed periods may be confined to the western part of the basin.

2) OCEAN DATA

Assessing the importance of MIF processes in the ocean is not straightforward. If the Gulf Stream current system and the North Atlantic mid-ocean behave in some analogous way to the numerical model flows, then the space and time statistics of the region several hundred kilometers south of the stream are needed to estimate an MIF forcing function. Then it is necessary to have oceanic statistics on the eddy field of a sort that can be compared with statistics computed from the response to the forcing function. Altogether too little data is available at this time to carry through such a procedure. However, some interesting data are available and will be briefly reviewed, with the MIF numbers from above in mind.

Near surface observations of the Gulf Stream have made it clear that there is considerable time dependence at periods longer than 7 days (Hansen, 1970; Robinson *et al.*, 1974), but there are not sustained observations sufficient to speak to the existence of significant transience at periods of several months or longer. Luyten (1977) has found strong transience with periods of $\lesssim$30 days under the Gulf Stream along the Continental Rise ~70°W, but also has too limited a time series to examine long period motions. The statistics of the southern "near field" of the Gulf Stream and the mid-ocean are known primarily through the work of Schmitz (1978). He presents the only available low-frequency spectra; these have not had the motions separated into a

TABLE 2. Eddy kinetic energy ($cm^2\ s^{-2}$) in different spectral bands from North Atlantic current meter data (Schmitz 1978).

Mooring	CM depth (m)	Period band (days) 100–1000	Period band (days) ~50–100
PMO8	600	~100	~300
PMO8	4000	~50	~130
MODE Center	500	~50	~25
MODE Center	4000	~2	~12

barotropic and baroclinic part, but the kinetic energy levels for the period bands 100–1000 and ~50–100 days at two different depths are useful (Table 2). From Table 2 it is seen that the kinetic energy levels at MODE Center (28°N, 70°W) are much lower than the corresponding values at PMO8 (37°30'N, 55°W). Further, the data suggest that there may be significant barotropic energy at PMO8 in both period bands.

These observations are difficult to apply directly to the MIF predictions because there is such a difference between baroclinic and barotropic forced response. If there is barotropic motion at the periods observed in the Gulf Stream and near field, the MIF theory predicts that energy could be radiated away in eddy-like motions. Radiation of baroclinic energy is much more uncertain. The relative lack of barotropic energy at MODE center can be explained only if the forcing function analogous to $f(x)$ is such that the eddy-like terms have rather small amplitude. Unfortunately, no information is available to estimate these amplitudes.

3) REMARKS

On the basis of the data and the very simple ideas here advanced, it appears possible for the MIF mechanism to operate in the ocean, at least for the barotropic mode. But too little information now exists about the variability of the ocean on periods of months and longer to say whether it is important or not. Many processes have also been omitted from this simple MIF theory which may profoundly alter the behavior of a forced solution in the oceanic context. Bottom topography, mean flows and nonlinear interactions may all alter the criteria for radiation of energy in something analogous to the "eddy-like" terms of (4). If the results presented here are found to be of interest many possibilities exist for beginning the exploration of the effects of these processes. For the reasons given in Section 1, attention has here been concentrated on the simplest system to yield results of interest.

Acknowledgments. We have enjoyed several very helpful discussions with D. Moore. DEH wishes also to acknowledge discussions with G. Flierl and J. Hirsh. This work was supported by the Office of Naval Research Contract N00014-76-C-0225 to Harvard University (DEH and ARR) and by National Science Foundation Grant 76-80210-OCE to MIT (DEH). This is POLYMODE Contribution No. 110.

REFERENCES

Dantzler, H. L., Jr., 1977: Potential energy maxima in the tropical and subtropical North Atlantic. *J. Phys. Oceanogr.*, **7**, 512–519.

Flierl, G. R., 1977: Simple application of McWilliams' "A note on a consistent quasigeostrophic model in a multiply connected domain. *Dyn. Atmos. Oceans*, **1**, 443–453.

——, V. M. Kamenkovich and A. R. Robinson, 1975: Gulf Stream meandering and Gulf Stream rings. Dynamics and the Analysis of MODE-1, MODE Dynamics Group, POLYMODE Office, Bldg. 54-1417, MIT (unpublished manuscript).

Haidvogel, D. B., and W. R. Holland, 1978: The stability of ocean currents in eddy-resolving general circulation models. *J. Phys. Oceanogr.*, **8**, 393–413.

Hansen, D., 1970: Gulf Stream meanders between Cape Hatteras and the Grand Banks. *Deep-Sea Res.*, **17**, 495.

Harrison, D. E., and A. R. Robinson, 1978: Energy analysis of open regions of turbulent flows-mean eddy energetics of a numerical ocean circulation experiment. *Dyn. Atmos. Oceans*, **2**, 185–211.

Holland, W. R., 1978: The role of mesoscale eddies in the general circulation of the ocean: Numerical experiments using a quasi-geostrophic model. *J. Phys. Oceanogr.*, **8**, 363–392.

——, and L. B. Lin, 1975: On the generation of mesoscale eddies and their contribution to the oceanic general circulation. Parts I and II. *J. Phys. Oceanogr.*, **5**, 642–669.

Ivanov, Yu. A., 1969: Characteristics of the propagation of disturbances on a bounded β-plane. *Izv. Atmos. Ocean. Phys.* **5**, 538–541.

Lin, L. B., 1974: A numerical study of mesoscale eddies in a two-layer wind-driven ocean. Ph.D. thesis, G.F.D. Program, Princeton University, 155 pp.

Luyten, J. R., 1977: Scales of motion in the deep Gulf Stream and across the continental rise. *J. Mar. Res.*, **35**, 49–74.

McWilliams, J. C., 1977: A note on a consistent quasigeostrophic model in a multiply connected domain. *Dyn. Atmos. Oceans*, **1**, 427–442.

MODE Group, 1978: The Mid-Ocean Dynamics Experiment. *Deep Sea Res.*, **25**, 859–910.

Pedlosky, J., 1977: On the radiation of mesoscale energy in the mid-ocean. *Deep-Sea Res.*, **24**, 591–600.

Philander, S. G. H., 1978: Forced oceanic waves. *Rev. Geophys. Space Phys.*, **16**, 15–46.

Rhines, P. B., 1977: The dynamics of unsteady currents. *The Sea*, Vol. 6, *Marine Modeling*, E. D. Goldberg, I. N. McCane, J. J. O'Brien and J. H. Steele, Eds. Wiley, 1049 pp.

Robinson, A. R., J. R. Luyten, and F. C. Fuglister, 1974: Transient Gulf Stream meandering Part I: An observational experiment. *J. Phys. Oceanogr.*, **4**, 237–255.

——, D. E. Harrison and D. B. Haidvogel, 1978: Mesoscale eddies and general ocean circulation models. *Dyn. Atmos. Oceans* (in press).

——, ——, Y. Mintz, and A. J. Semtner, Jr., 1977: Eddies and the general circulation of an idealized ocean gyre: A wind and thermally driven primitive equation numerical experiment. *J. Phys. Oceanogr.*, **7**, 182–207.

Schmitz, W. J., Jr., 1977: On the deep general circulation of the western North Atlantic. *J. Mar. Res.*, **35**, 21–28.

——, 1978: Observations of the vertical distribution of low-frequency kinetic energy in the western North Atlantic. *J. Mar. Res.*, **36**, 295–310.

Semtner, A. J., Jr., and Y. Mintz, 1977: Numerical simulation of the Gulf Stream and ocean eddies. *J. Phys. Oceanogr.*, **7**, 208–230.